Ab initio study of Pb antisite defects in $PbZrO_3$ and $Pb(Zr,Ti)O_3$

R. Kagimura
Materials Science and Technology Division, Oak Ridge National Laboratory, Oak Ridge, Tennessee 37831-6114, USA and Department of Physics and Astronomy, University of Tennessee, Knoxville, Tennessee 37996-1200, USA

D. J. Singh
Materials Science and Technology Division, Oak Ridge National Laboratory, Oak Ridge, Tennessee 37831-6114, USA

(Received 7 March 2008; revised manuscript received 29 September 2008; published 7 November 2008)

We report an *ab initio* study of Pb antisite defects in $PbZrO_3$ (PZ) and $Pb(Zr,Ti)O_3$ (PZT) perovskites. Also, we calculated the enthalpy of formation of PZ. Our results show that, under strong oxidizing conditions, Pb on the Zr-site antisite defects are unavoidable in PZ. Moreover, a positive enthalpy of formation (0.15 eV) of PZ is found. This indicates that PZ is metastable for low temperature and may help explain the difficulty in synthesizing high-quality Zr-rich PZT crystals. The Pb antisite defects in PZT alloys have low formation energies. This result is in agreement with experiments, which report the predominance of this defect in PZT films. We find that the Pb antisite defect produces electron traps 0.2–0.8 eV below the conduction-band edge.

DOI: 10.1103/PhysRevB.78.174105 PACS number(s): 77.84.Dy, 71.15.Mb

I. INTRODUCTION

Pb-based perovskite materials, especially lead zirconate titanate (PZT), are widely used in electronic devices and in other technological applications due to their piezoelectric, ferroelectric, and dielectric properties.[1–3] PZT solid solutions with compositions near the so-called morphotropic phase boundary,[1] which separates the rhombohedral and tetragonal ferroelectric phases, have been the focus of intense investigations for many years.[4] However, the investigation of the Zr-rich region of the PZT phase diagram is also interesting; for example, the study of the phase transition from the low temperature to the high-temperature rhombohedral phases may be useful in development of thermal detectors.[5] Also, the end-point compound of the Zr-rich region, $PbZrO_3$, may have a positive enthalpy of formation from the PbO and ZrO_2 binary oxides. High-temperature solution calorimetry measurements[6] find a positive heat of formation, 1.7 ± 6.6 KJ/mol, of $PbZrO_3$ (PZ) from binary compounds at 1068 K. Also, empirical estimates[7] yield a positive heat of formation for this material. These results indicate that PZ is metastable for low temperature and could explain the difficulty of synthesizing high-quality pure PZT crystals for Zr-rich compositions. Understanding the difficulty in making PZT crystals is an important issue because perovskite crystals normally have far superior piezoelectric properties than ceramics.

In any case, based on those results, intrinsic defects may be expected in PZ and Zr-rich PZT perovskites. Also, to compensate the lead loss and to enhance the crystallization of PZT, a lead excess is normally required during the Pb-based perovskite growth processes.[8] Therefore, one possible intrinsic defect that can be present in Pb-based perovskite is the Pb antisite defect. In fact, experimental investigation in $Pb(Sc_{1/2}Ta_{1/2})O_3$ (Ref. 9) suggests, by several arguments, that the lead excess used during the growth processes may be located at the B-site of the perovskite structure. Also, recent experiments[10,11] have reported the presence of Pb antisite defects in PZT, forming a $PbZrO_3$-$PbTiO_3$-$PbPbO_3$ solid solution. In addition, experimental results[11] suggest that the antisite defect Pb atom on the Zr site (Pb_{Zr}) is more common than the Pb on the Ti site (Pb_{Ti}) in PZT films, based on a ternary phase diagram.[11,12] The purpose of this paper is to investigate the enthalpy of formation of $PbZrO_3$, and study the Pb antisite defects energies and their effects on the electronic structure and on the total polarization in PZ and PZT perovskites. In this study, we have considered for the formation energy calculations, strongly oxidizing conditions, where the Pb, Zr, and Ti fully oxidized compounds are used as the reservoir. This is a reasonable assumption, since in the experimental works the PZT thin films were grown in a pure oxygen atmosphere at 0.02 mbar[10,13] and in an argon/oxygen atmosphere at 0.02–0.04 mbar.[11]

We used density-functional supercell calculations for $PbZrO_3$ perovskite, and for $Pb(Zr_{1/2}Ti_{1/2})O_3$ (PZT50/50) and $Pb(Zr_{3/4}Ti_{1/4})O_3$ (PZT75/25) solid solution with different configurations for the Zr and Ti atoms. Our results indicate that PZ is metastable for low temperature and the antisite defects are unavoidable in this material. The Pb antisite defects in PZT50/50 present low formation energies and they are unavoidable in PZT75/25, especially the Pb_{Zr} defects, which is in agreement with experiments.[11] Finally, are find electron traps 0.2–0.8 eV below the conduction-band minimum in PZT supercells with Pb antisites defects, depending on the compositions.

II. FIRST-PRINCIPLES CALCULATIONS

We used density-functional theory (DFT)[14] and the local-density approximation (LDA).[15] To calculate the total energies we have used a general potential linearized augmented plane-wave (LAPW) method[16] with local orbitals[17] as implemented in our in-house code. We used the following LAPW sphere radii: 1.90, 1.90, 1.80, and 1.50 a.u. for Pb, Zr, Ti, and O, respectively. Regarding the basis set, we used local orbitals and LAPW functions with cutoff $RK_{max}=7.0$, where R is the smallest LAPW sphere radius. The supercell approach was used with 40 atoms to represent the PZ and PZT structures. 40 atom cells are the minimum size that can accom-

modate the various Glazer tilt systems in perovskites. The Brillouin-zone samplings were done using **k** points[18] meshes of $2\times2\times2$, $4\times2\times4$, and $6\times6\times6$ for PZT, orthorhombic PZ, and binary compounds, respectively. The total-energy differences are converged in relation to the computational parameters to a precision of 1 mRy. Experimental lattice parameters[5,19–24] were used in our investigations, but all atomic positions were fully relaxed. Also, we calculated the total electric polarization of the PZT alloys with the Berry phase approach[25] using a pseudopotential[26] method, as implemented in the ABINIT code.[27] For the basis set, we used plane waves with a cutoff energy of 45 hartree. However, Berry phase calculations give the polarization with the ambiguity that an arbitrary number of polarization quanta $2e/a^2$ (a is the lattice parameter) may be added. Considering that these quanta are small for supercells, we also estimated the polarization by computing the dispacement of each cation from the center of its anion cage and multiplying by the Born effective charges, also determined by linear response. In this way the number of polarization quanta was determined. This was not zero, but rather one along the polarization direction for the ferroelectric supercells. Finally, we note that for these calculations we used the optimized atomic positions obtained from the LAPW calculations.

The structure of $PbZrO_3$ has been investigated by many experimental works[19,28] as well as by LDA calculations.[29,30] An agreement between theoretical and experimental results has been established. The PZ ground-state structure, which is orthorhombic and has 40 atoms per unit cell, and its relation to the "perfect cubic cell" are discussed in our previous work.[31] For the PZT structure, we focus on the Zr-rich region of the PZT phase diagram,[1] where PZT has a rhombohedral structure for a wide range of Ti concentration. Here we represent the alloys with 40 atom supercells defined by the lattice vectors (2, 0, 0)a, (0, 2, 0)a, and (0, 0, 2)a, in the pseudocubic coordinate system. The lattice constant "a" for the PZT50/50 and PZT75/25 cells are obtained by constraining the volume of these cells per formula unit to be equal to the experimental volume of the $Pb(Zr_{0.52}Ti_{0.48})O_3$ [20] tetragonal and $Pb(Zr_{0.77}Ti_{0.23})O_3$ [5] rhombohedral lattices, respectively. We have neglected the rhombohedral strain in our calculations, which is small.[5] For the binary compounds we optimize the atomic positions starting from the experimental ones. No symmetry constraints were imposed for the relaxation of the atomic positions in any of the cells. The experimental lattice constants used in our calculations are shown in the Table I.

TABLE I. Experimental lattice constants, in angstrom, for PZ, PZT77/23, PZT52/48, PbO, PbO_2, TiO_2, and ZrO_2, and the monoclinic angle (β), in degree, for ZrO_2 used in our calculations.

	a	b	c	β	Ref.
PZ	8.2077	11.7742	5.8752		19
PZT77/23	5.8134		14.3500		5
PZT52/48	4.044	4.044	4.138		20
PbO	3.96	3.96	5.01		21
PbO_2	4.9578	4.9578	3.3878		22
TiO_2	4.5937	4.5937	2.9587		23
ZrO_2	5.1505	5.2116	5.3173	99.230	24

III. RESULTS AND DISCUSSION

First, we discuss the heat of formation of $PbZrO_3$ from binary compounds. We consider the following reaction:

$$PbO + ZrO_2 \rightarrow PbZrO_3. \quad (1)$$

Now, the heat of formation, H_{form}, can be defined as:

$$H_{form} = E^{PZ} - E^{PbO} - E^{ZrO_2}, \quad (2)$$

where E^{PZ}, E^{PbO}, and E^{ZrO_2} are the total energies of the $PbZrO_3$, PbO, and ZrO_2 compounds, respectively. Here, we used the tetragonal (space-group $P4/nmm$) and monoclinic (space-group $P2_1/c$) structures for the PbO and ZrO_2 compounds, respectively. Our LDA calculated atomic positions are in good agreement with the experimental ones, as shown in Table II.

Our results show that the heat of formation for $PbZrO_3$ from binary compounds is positive, by 0.15 eV. This result indicates that $PbZrO_3$ is metastable at low temperature. As mentioned, there are experimental indications of this as well, both from empirical estimates, which yield 0.14 eV,[7] and high-temperature calorimetric measurements, which yield $H_{form}(1068\ K)=0.02$ eV.[6]

The above results indicate that intrinsic defects can be expected in PZ and in rhombohedral PZT, especially antisite defects, as mentioned. Based on that, we calculated the formation energy of Pb antisite defects in PZ, and in PZT with composition of Zr/Ti atoms of 50%/50% (PZT50/50) and 75%/25% (PZT75/25). For PZT50/50, we have considered three different orderings for the B-site atoms in the supercell: fcc order (G-type), chain order along the [001] direction of the pseudocubic (C-type), and a layered order perpendicular to the [001] direction of the pseudocubic (A-type). The variation in properties between these different supercells shows the size of the effects that can be expected due to different

TABLE II. Calculated and experimental (Exp.) fractional atomic coordinates for monoclinic ZrO_2 (space-group $P2_1/c$), and the Pb positional parameter, referred to the lattice vectors, for tetragonal PbO (space group $P4/nmm$).

		ZrO_2	ZrO_2(Exp.[a])			PbO	PbO(Exp.[b])
Zr	x	0.276	0.2754	Pb	z	0.237	0.237
	y	0.043	0.0395				
	z	0.209	0.2083				
O1	x	0.067	0.0700				
	y	0.330	0.3317				
	z	0.348	0.3447				
O2	x	0.451	0.4496				
	y	0.757	0.7569				
	z	0.478	0.4792				

[a]Ref. 24.
[b]Ref. 21.

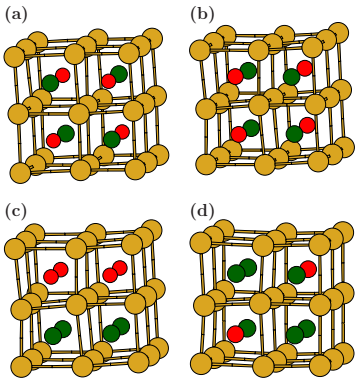

FIG. 1. (Color online) Different orderings for the *B*-site atoms of $Pb(Zr_{1/2}Ti_{1/2})O_3$: (a) fcc order (*G* type), (b) chain order (*C* type), and (c) layered order (*A* type). In (d), we show the $Pb(Zr_{3/4}Ti_{1/4})O_3$ structure we considered. The yellow, green, and red circles represent the Pb, Zr, and Ti atoms, respectively. The oxygen atoms are not shown.

local cation environments in the PZT alloy. For PZT75/25, we consider the B-site configuration where the Ti atoms are arranged as far apart in space as possible, since the Ti concentration is low. These orderings are shown in the Fig. 1.

To investigate the energetics of Pb antisite defects, we calculate the total energies (E^{Bulk}) for PZ and PZT free-defect supercells, allowing a full relaxation of the atomic positions. Replacing one B-site atom of those optimized free-defect supercells by a Pb atom, and allowing a full relaxation of atomic positions, we can calculate the Pb antisite defect formation energy using

$$E_{form}^{Pb_{Zr}} = E^{Def} - E^{Bulk} - E^{PbO_2} + E^{ZrO_2}, \quad (3)$$

$$E_{form}^{Pb_{Ti}} = E^{Def} - E^{Bulk} - E^{PbO_2} + E^{TiO_2}, \quad (4)$$

where $E_{form}^{Pb_{Zr}}$ ($E_{form}^{Pb_{Ti}}$) is the defect formation energy of a Pb on the Zr (Ti) site, E^{Def} is the total energy of a supercell containing a Pb antisite defect, E^{PbO_2}, E^{ZrO_2}, and E^{TiO_2}, are the total energies of PbO_2, ZrO_2, and TiO_2 compounds, respectively. Here, we consider the fully oxidized Pb, Ti, and Zr compounds as the reservoir. The calculated oxygen positional parameters (u) for TiO_2 and PbO_2 are 0.305 and 0.307, respectively. Our results are similar to the experimental data,[22,23] $u_{TiO_2}=0.3048$ and $u_{PbO_2}=0.3067$.

Our calculated defect formation energies for PZ and PZT are shown in the Table III. For PZT50/50 we consider an average of the defect formation energies for the G-type, C-type, and A-type B-site configurations, also shown in the Table III. Our calculations show that under strong oxidizing conditions and low temperature the Pb antisite defects are unavoidable in PZ and Zr-rich PZT. This can be related to the positive heat of formation. Also, Pb antisite defects present a low formation energy in PZT50/50, and the Pb atom on the Zr site is energetically more favorable than the Pb atom on the Ti site. We note that the Shannon ionic radius[32] of Pb^{4+} is closer to that of Zr^{4+} than Ti^{4+}. Within our finite-size supercells strain effects would therefore favor replacement of a Zr rather than a Ti by Pb. In a real alloy, such effects would also presumably play a role favoring antisites coordinated by Ti neighbors to reduce local strain.

TABLE III. Calculated formation energy, in electron volts, of Pb antisite defects of PZ, PZT50/50, and PZT75/25. For PZT50/50, an average of the defect formation energies for the *G*-type, *A*-type, and *C*-type *B*-site configurations is shown.

	PZ	PZT75/25	PZT50/50	*G* type	*A* type	*C* type
Pb_{Zr}	−0.18	−0.09	0.02	0.00	0.04	0.01
Pb_{Ti}		−0.05	0.15	0.20	0.09	0.16

TABLE IV. Calculated total polarization, in $\mu C/cm^2$, for perfect PZT alloys and for supercells containing a Pb antisite defect.

	PZ	PZT75/25	*A* type	*C* type	*G* type
Perfect	0	65	54	61	63
Pb_{Zr}	2	71	53	66	66
Pb_{Ti}		71	66	67	68

To study the impact of the Pb antisite defects on the local structure, we have calculated the off centerings of Pb, Zr, Ti atoms in relation to their oxygen cages for the "perfect" and "defective" PZ and PZT supercells. Our calculated off centerings indicate that the maximum displacement of the substitutional Pb atom is 0.09 Å (0.25 Å) in relation to the off centering of the replaced Zr (Ti) atom for PZ and PZT. Also, the other Pb atoms of the supercells containing the Pb_{Zr} (Pb_{Ti}) defects displace ≈0.10 Å (0.25 Å) for PZ and PZT50/50 and ≈0.20 Å (0.70 Å) for PZT75/25 in relation to the off centerings of the Pb atoms of the perfect cell. Also, it may be expected that changes in the displacement of Pb atoms can affect the total polarization of these systems. To investigate that, we have calculated the total electric polarization for the perfect and defect containing PZ and PZT supercells. The calculated polarizations are shown in the Table IV. We observe that for 40 atom supercells the Pb antisite defects generally modestly increase the total polarization in relation to that of the perfect cell, with the sole exception of the Pb_{Zr} defect in the A-type PZT supercell. Therefore, higher polarization may be expected in thin-film samples that are grown under conditions favoring Pb antisites. In general the properties of PZT alloys are given by an average over Zr/Ti configurations. However, recent developments in thin-film synthesis allow artificially ordered structures to be grown. In that case, perhaps the sensitivity of the effect of antisites to cation ordering as shown in the table can be used to modify the properties of such films.

Finally, in order to investigate in more detail the effect of the Pb substitutional atom on the B-site, we calculate the total density of states (DOS) for the defect-free PZ and PZT supercells, and for supercells containing the antisite defects. Our calculated DOS are shown in the Fig. 2. These show the presence of trap states in the energy gap below the conduction-band minimum, by 0.2–0.8 eV (depending on ordering and composition). This state has an s character due to the Pb atom at the B-site, as shown in the Fig. 3.

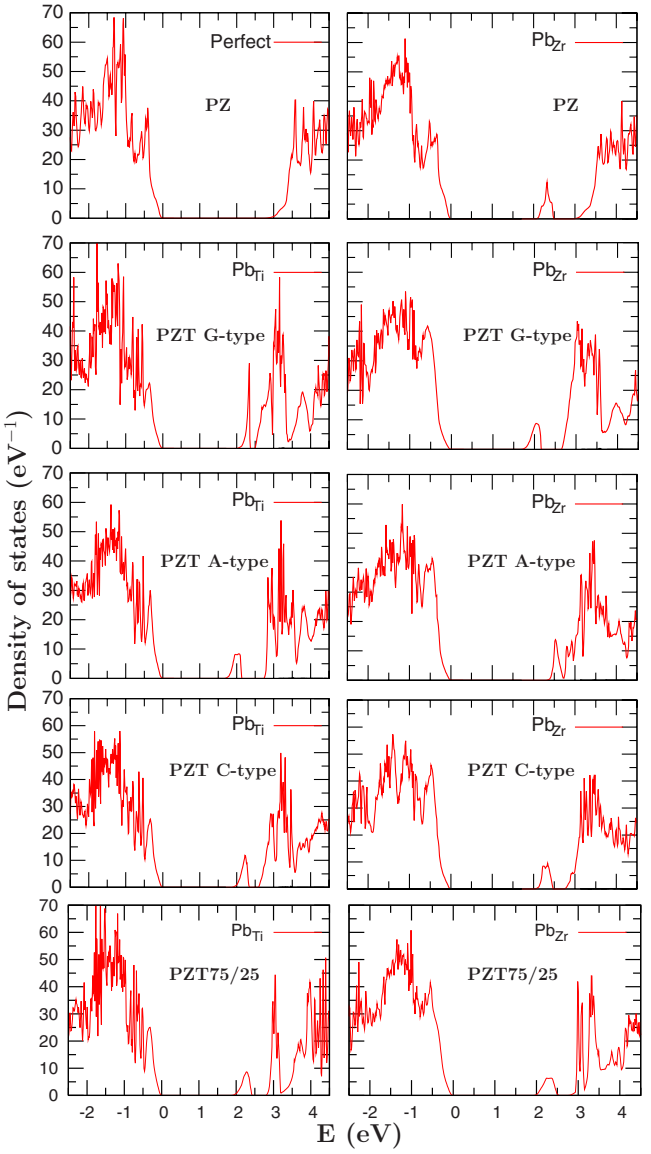

FIG. 2. (Color online) Calculated electronic total densities of states against the energy of 40 atom supercells of PZ, PZT50/50, and PZT75/25. The panels show the total densities of states of the perfect PZ structure, and the PZ and PZT supercells containing Pb_{Zr} and Pb_{Ti} antisite defects. The Fermi level is the reference of energy.

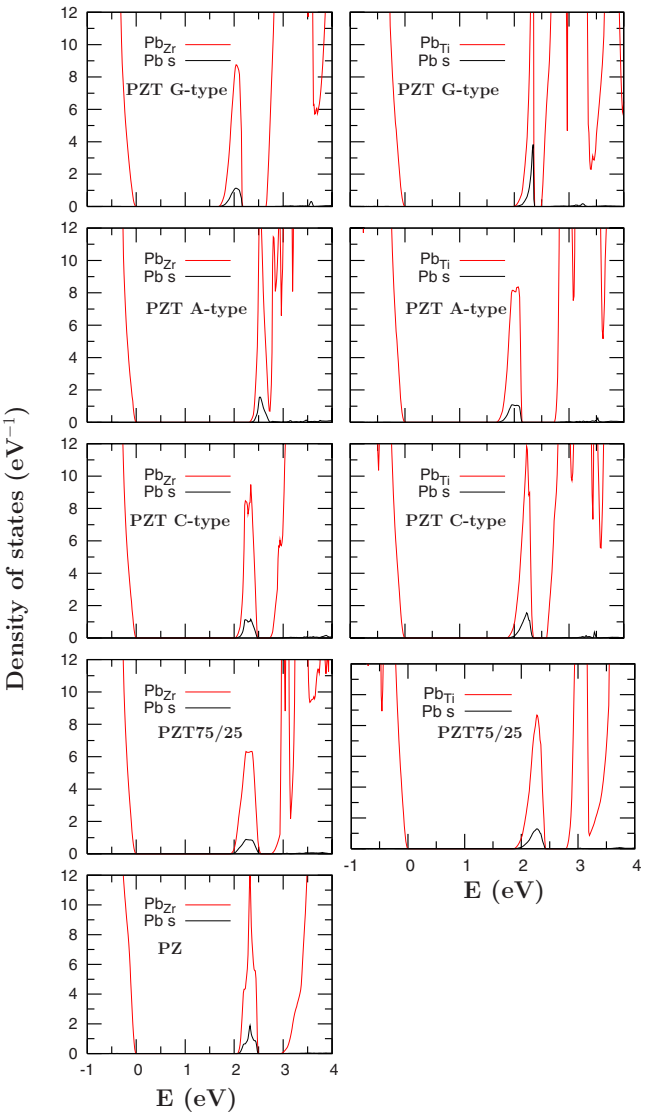

FIG. 3. (Color online) Calculated partial densities of states from the Pb atom on the *B* site with *s* character against the energy of 40 atom supercells of PZ and PZT.

IV. CONCLUSIONS

In summary, in this work we have investigated the heat of formation of $PbZrO_3$ from binary compounds, and the energetics of antisite defects and the effects on the electronic structure in PZ and PZT perovskites. Our results show a positive value for the heat of formation of PZ, indicating that this material is metastable for low temperature. The calculated Pb antisite defect formation energies show that, under strong oxidizing conditions, Pb antisite defects are unavoidable in PZ and PZT75/25 and have a low formation energy for PZT50/50. The calculated densities of states for PZ and PZT show trap states near the conduction-band minimum. Spectroscopy of these defect states may be useful in characterizing these PZT samples.

ACKNOWLEDGMENTS

This work was supported by the Department of Energy ORNL LDRD program and Division of Materials Science and Engineering, and by the Office of Naval Research. One of the authors (R.K.) also was supported by the Brazilian agency—CNPq (Conselho Nacional de Desenvolvimento Científico e Tecnológico).

[1] B. Jaffe, W. R. Cook, and H. Jaffe, *Piezoelectric Ceramics* (Academic, New York, 1971).
[2] K. Uchino, *Piezoelectric Actuators and Ultrasonic Motors* (Kluwer, Dordrecht, 1971).
[3] E. Cross, Nature (London) **432**, 24 (2004).
[4] B. Noheda, Curr. Opin. Solid State Mater. Sci. **6**, 27 (2002), and references therein.
[5] D. L. Corker, A. M. Glazer, R. W. Whatmore, A. Stallard, and F. Fauth, J. Phys.: Condens. Matter **10**, 6251 (1998).
[6] E. Takayama-Muromachi and A. Navrotsky, J. Solid State Chem. **72**, 244 (1988).
[7] M. M. Lencka and R. E. Riman, Thermochim. Acta **256**, 193 (1995).
[8] W. Zhang, K. Sasaki, and T. Hata, Jpn. J. Appl. Phys., Part 1 **35**, 1868 (1996).
[9] R. W. Whatmore, Z. Huang, and M. Todd, J. Appl. Phys. **82**, 5686 (1997).
[10] P. Muralt, S. Hiboux, C. Mueller, T. Maeder, L. Sagalowicz, T. Egami, and N. Setter, Integr. Ferroelectr. **36**, 53 (2001).
[11] G. Suchaneck, A. Deyneka, L. Jastrabik, M. Savinov, and G. Gerlach, Ferroelectrics **318**, 3 (2005).
[12] By Zr and Ti sites in an alloy one means sites in Ti and Zr-rich local environments, respectively.
[13] S. Hiboux, P. Muralt, and T. Maeder, J. Mater. Res. **14**, 4307 (1999).
[14] W. Kohn and L. J. Sham, Phys. Rev. **140**, A1133 (1965).
[15] L. Hedin and B. I. Lundqvist, J. Phys. C **4**, 2064 (1971).
[16] D. J. Singh and L. Nordstrom, *Planewaves, Pseudopotentials, and the LAPW Method*, 2nd ed. (Springer, New York, 2006).
[17] D. J. Singh, Phys. Rev. B **43**, 6388 (1991).
[18] H. J. Monkhorst and J. D. Pack, Phys. Rev. B **13**, 5188 (1976).
[19] H. Fujishita, Y. Ishikawa, S. Tanaka, A. Ogawaguchi, and S. Katano, J. Phys. Soc. Jpn. **72**, 1426 (2003).
[20] B. Noheda, J. A. Gonzalo, L. E. Cross, R. Guo, S.-E. Park, D. E. Cox, and G. Shirane, Phys. Rev. B **61**, 8687 (2000).
[21] J. Leciejewicz, Acta Crystallogr. **14**, 1304 (1961).
[22] P. D'Antonio and A. Santoro, Acta Crystallogr., Sect. B: Struct. Crystallogr. Cryst. Chem. **36**, 2394 (1980).
[23] S. C. Abrahams and J. L. Bernstein, J. Chem. Phys. **55**, 3206 (1971).
[24] C. J. Howard, R. J. Hill, and B. E. Reichert, Acta Crystallogr., Sect. B: Struct. Sci. **44**, 116 (1988).
[25] R. D. King-Smith and D. Vanderbilt, Phys. Rev. B **47**, 1651 (1993).
[26] N. Troullier and J. L. Martins, Phys. Rev. B **43**, 1993 (1991).
[27] X. Gonze *et al.*, Comput. Mater. Sci. **25**, 478 (2002); X. Gonze *et al.*, Z. Kristallogr. **220**, 558 (2005).
[28] H. Fujishita and S. Katano, J. Phys. Soc. Jpn. **66**, 3484 (1997), and references therein.
[29] D. J. Singh, Phys. Rev. B **52**, 12559 (1995).
[30] M. D. Johannes and D. J. Singh, Phys. Rev. B **71**, 212101 (2005).
[31] R. Kagimura and D. J. Singh, Phys. Rev. B **77**, 104113 (2008).
[32] R. D. Shannon, Acta Crystallogr., Sect. A: Cryst. Phys., Diffr., Theor. Gen. Crystallogr. **32**, 751 (1976).